HHS Public Access

Author manuscript

Nat Microbiol. Author manuscript; available in PMC 2021 June 03.

Published in final edited form as:

Nat Microbiol. 2021 January ; 6(1): 11–18. doi:10.1038/s41564-020-00835-2.

Therapeutically Administered Ribonucleoside Analogue MK-4482/EIDD-2801 Blocks SARS-CoV-2 Transmission in Ferrets

Robert M. Cox[1,#], **Josef D. Wolf**[1,#], **Richard K. Plemper**[1,*]

[1]Institute for Biomedical Sciences, Georgia State University, Atlanta, GA

The coronavirus disease (COVID)-19 pandemic is having a catastrophic impact on human health[1]. Widespread community transmission has triggered stringent distancing measures with severe socioeconomic consequences. Gaining control of the pandemic will depend on interruption of transmission chains until vaccine-induced or naturally-acquired protective herd immunity arises. However, approved antiviral treatments such as remdesivir and reconvalescent serum cannot be delivered orally[2,3], making them poorly suitable for transmission control. We previously reported development of an orally efficacious ribonucleoside analogue inhibitor of influenza viruses, MK-4482/EIDD-2801[4,5], that was repurposed against SARS-CoV-2 and is currently in phase II/III clinical trials (NCT04405570 and NCT04405739). In this study, we explored efficacy of therapeutically administered MK-4482/EIDD-2801 to mitigate SARS-CoV-2 infection and block transmission in the ferret model, since ferrets and related members of the weasel genus transmit the virus efficiently with minimal clinical signs[6–9], which resembles spread in the human young-adult population. We demonstrate high SARS-CoV-2 burden in nasal tissues and secretions that coincided with efficient direct-contact transmission. Therapeutic treatment of infected animals with twice-daily MK-4482/EIDD-2801 significantly reduced upper respiratory tract SARS-CoV-2 load and completely suppressed spread to untreated

[*]to whom correspondence should be addressed: rplemper@gsu.edu.

Author contributions

RMC and JDW performed virus stock preparations, animal inoculation, sampling and necropsies, contributed to experiment design, data analysis and presentation, and edited the manuscript. RMC performed all RT-qPCR experiments and analyses. JDW performed all CBC analyses. RKP conceived, designed and coordinated the study, conceived and designed experiments, contributed to animal inoculation and necropsies, contributed to data analysis and presentation, and wrote the manuscript.

[#]these authors contributed equally to this work

Competing interests

The authors declare no competing interests.

Ethics statement

All animal work was performed in compliance with the *Guide for the Care and Use of Laboratory Animals* of the National Institutes of Health and the Animal Welfare Act Code of Federal Regulations. Experiments with SARS-CoV-2 involving ferrets were approved by the Georgia State Institutional Animal Care and Use Committee under protocol A20031. All experiments using infectious SARS-CoV-2 were approved by the Georgia State Institutional Biosafety Committee under protocol B20016 and performed in a BSL-3/ABSL-3 facilities at Georgia State University.

Data availability statement

All data generated or analyzed during this study are included in this published article. Source data for Figures 1–3 and Extended Data 1–4 is provided in the Source Data files associated with the individual figures.

Code availability statement

This study does not use custom codes. All commercial computer codes and algorithms used are specified in the Methods section.

contact animals. This study identified oral MK-4482/EIDD-2801 as a promising antiviral countermeasure to break SARS-CoV-2 community transmission chains.

MK-4482/EIDD-2801 is the orally available pro-drug of the nucleoside analogue N^4-hydroxycytidine (NHC), which has shown potent anti-influenza virus activity in mice, guinea pigs, ferrets, and human airway epithelium organoids[4,10,11]. Acting through induction of error catastrophe in virus replication[4,12], NHC has broad-spectrum anti-RNA virus activity. In addition to ameliorating acute disease, we have demonstrated in a guinea pig transmission model that NHC effectively blocks influenza virus spread from infected animals to untreated contact animals[11].

Several mouse models of SARS-CoV-2 infection have been developed, some of which were employed to confirm *in vivo* efficacy of MK-4482/EIDD-2801 also against betacoronaviruses[13]. However, human SARS-CoV-2 cannot productively infect mice without viral adaptation or introduction of human ACE2 into transgenic animals, and none of the mouse models supports transmission to uninfected mice[14]. Spill-back of SARS-CoV-2 to farmed minks, subsequent large-scale mink-to-mink transmission and, in some cases, zoonotic transmission back to humans revealed efficient viral spread among members of the weasel genus without prior adaptation[6–9]. Although mink farms reported elevated animal mortality and gastrointestinal and respiratory clinical signs[15], outbreak follow-up revealed continued intra-colony spread for extended periods of time[9], suggesting that acute clinical signs in the majority of infected animals may be mild. These mink field reports corroborated results obtained with experimentally infected ferrets showing that mustelids of the weasel genus transmit SARS-CoV-2 efficiently without strong clinical disease manifestation[16,17]. Since this presentation of SARS-CoV-2 infection resembles the experience of frequently asymptomatic or mildly symptomatic SARS-CoV-2 spread in the human young-adult population[18], ferrets represent a relevant model species to assess therapeutic impact on SARS-CoV-2 transmission.

To first validate host invasion and tissue tropism of SARS-CoV-2 in ferrets, we inoculated animals intranasally with 1×10^4 or 1×10^5 plaque-forming units (pfu) of SARS-CoV-2 clinical isolate 2019-nCoV/USA-WA1/2020 per animal. Shed virus burden was monitored daily over a 10-day period. Virus load in the upper and lower respiratory tract was determined in two animals of each inoculum group on days four and ten after infection, respectively.

In animals of the high inoculum group, virus release from the upper respiratory tract peaked three days after infection and was undetectable by day seven (Fig. 1a; Supplementary Table 1). Infection of animals in the low inoculum group was less efficient. Shedding profiles closely correlated with infectious particle load in nasal turbinates; a heavy virus tissue burden in the high inoculum group was present on day 4, which greatly decreased by approximately four orders of magnitude by day 10 (Fig. 1b; Supplementary Table 2).

Low inoculum resulted in light virus load in the turbinates on day 4 and undetectable burden thereafter. However, qPCR-based quantitation of viral RNA copy numbers in the turbinates revealed continued presence of a moderate (approx. 10^4 copies/g tissue) to high ($\geq10^7$

copies/g tissue) virus load after low and high inoculum, respectively (Fig. 1c; Supplementary Table 3). Independent of inoculum amount, no infectious particles were detected in bronchoalveolar lavages or lung tissue samples (Extended Data 1). At both days 4 and 10, several organ samples (lung, heart, kidney, liver) were also qPCR-negative (Fig. 1d), confirming inefficient infection of the ferret lower respiratory tract and limited systemic host invasion. Only small and large intestine samples were PCR-positive on day 4 after infection, and rectal swabs showed continued low-grade shedding of viral genetic material (Fig. 1e; Supplementary Table 4).

Animals in the high-inoculum group experienced a transient drop in bodyweight that reached a low plateau on days 5–6 after infection, but fully recovered by the end of study (Fig. 1f; Supplementary Table 5). One animal of the low-inoculum group showed a gradual, slight reduction in body weight until study end (day 10). No other clinical signs such as fever or respiratory discharge were noted. Complete blood counts taken every second day revealed no significant deterioration from the normal range in either inoculum group in overall white blood cells counts and lymphocyte, neutrophil, and platelet populations (Fig. 1g; Supplementary Table 6). Relative expression levels of type I and II interferon in ferret peripheral blood mononuclear cells (PBMCs) sampled in 48-hour intervals reached a plateau approximately 3 days after infection and stayed moderately elevated until the end of the study (Fig. 1h–I; Supplementary Table 7). In some animals, IL-6 levels were moderately elevated, but changes did not reach statistical significance (Fig. 1j). However, we noted a prominent expression peak of selected interferon-stimulated genes (ISGs) with antiviral effector function (MX1 and ISG15) four days after infection, followed by return to baseline expression by study end (Fig. 1k–l).

Prior to *in vivo* efficacy evaluation, we validated the potency of NHC against SARS-CoV-2 clinical isolate 2019-nCoV/USA-WA1/2020 in cell culture (Fig. 2a). Four-parameter variable slope regression modeling of dose-response data revealed 50% and 90% effective concentrations of approximately 3.4 μM and 5.4 μM, respectively, which is within an approximately 6-fold range of potency data reported for other human betacoronaviruses[19]. Based on these results, ferrets were infected in subsequent MK-4482/EIDD-2801 efficacy tests with 1×10^5 pfu/animal and infectious virions in nasal lavages determined twice daily (Fig. 2b). Viral burden in respiratory tissues was assessed four days after infection. In all treatment experiments, MK-4482/EIDD-2801 was administered twice daily (*b.i.d.*) through oral gavage. Dosing commenced 12 hours after infection at 5 or 15 mg/kg bodyweight, or 36 hours after infection at 15 mg/kg. Shed viral titers in nasal lavages were equivalent in all MK-4482/EIDD-2801 groups and vehicle-treated controls at the time of first treatment start (12 hours after infection), indicating uniform inoculation of all animals in the study (Fig. 2c; Extended Data 2a). Initiation of therapy at the 12-hour time point resulted in a significant reduction ($p<0.001$) of shed virus load within 12 hours, independent of the MK-4482/EIDD-2801 dose level administered, and infectious particles became undetectable within 24 hours of treatment start. When first administered at the peak of virus shedding (36 hours after infection), MK-4482/EIDD-2801 completely suppressed release of infectious virions into nasal lavages within a slightly longer 36-hour period, whereas vehicle control animals continued to shed infectious particles until study end.

By 3.5 days after infection, only vehicle-treated animals carried detectable virus burden in nasal turbinates (Fig. 2d; Extended Data 2b), indicating that MK-4482/EIDD-2801 had silenced all SARS-CoV-2 replication. SARS-CoV-2 RNA was still detectable in nasal tissues extracted from animals of all groups, albeit significantly reduced ($p=0.0089$ and $p=0.0081$ for the 5 mg/kg and 15 mg/kg MK-4482/EIDD-2801 groups, respectively) in treated animals versus the vehicle controls (Fig. 2e; Extended Data 2c). Animals of the 12-hour therapeutic groups showed a significant reduction ($p\leq0.044$) in effector ISG expression compared to vehicle-treated animals, although no significant differences in relative interferon and IL-6 induction were observed (Extended Data 3a–f).

These results demonstrate oral efficacy of therapeutically administered MK-4482/EIDD-2801 against acute SARS-CoV-2 infection in the ferret model. Consistent with our previous pharmacokinetic (PK) and toxicology work-up of MK-4482/EIDD-2801 in ferrets, treatment did not cause any phenotypically overt adverse effects and white blood cell and platelet counts of drug-experienced animals remained in the normal range (Extended Data 4).

SARS-CoV-2 shedding into the ferret upper respiratory tract establishes conditions for productive spread from infected source to uninfected contact animals[16,17]. To assess transmission efficiency, we co-housed intranasally infected source animals with two uninfected contact animals each for a 3-day period, starting 30 hours after source animal inoculation (Fig. 3a). Nasal lavages and rectal swabs were obtained from all animals once daily and blood sampled at study start and on days four and eight after the original infection. Viral burden and RNA copy numbers in respiratory tissues were determined at the end of the co-housing phase (source animals) and at study end (contact animals).

Infectious particles first emerged in nasal lavages of some contact animals 24 hours after the start of co-housing (Fig. 3b; Supplementary Table 8). By the end of the co-housing phase, all contact animals were infected and approached peak virus replication phase, demonstrating that SARS-CoV-2 transmission among ferrets is rapid and highly efficient.

A second cohort of source animals inoculated in parallel with SARS-CoV-2 received oral MK-4482/EIDD-2801 at the 5 mg/kg bodyweight dose level, administered *b.i.d.* starting 12 hours after infection. Productive infection of these animals was validated by SARS-CoV-2 titers in nasal lavages one day after infection (Fig. 3b) that very closely matched those seen in the initial efficacy tests (Fig. 2c). Although we also co-housed the treated source animals for nearly 3 days with two untreated contacts each, no infectious SARS-CoV-2 particles were detected in any of the series of nasal lavages obtained from these contacts throughout the study or in any of the contact animal nasal turbinates sampled at study end (Fig. 3c; Supplementary Table 9).

Nasal turbinates extracted from the contacts of vehicle-treated source animals contained high viral RNA copy numbers, underscoring successful host invasion after transmission (Fig. 3d; Supplementary Table 10). Consistent with our earlier observations, turbinates of treated source animals harbored moderate to high ($\geq10^5$ copies/g tissue) amounts of viral RNA although infectious particles could not be detected. In contrast, all respiratory tissues of the

contacts co-housed with MK-4482/EIDD-2801-treated source animals remained SARS-CoV-2 genome free, indicating the absence of any low-grade virus replication that could have hypothetically progressed in these animals below the detection level of infectious particles (Fig. 3e,f; Supplementary Tables 11 and 12). Low SARS-CoV-2 RNA copy numbers were furthermore present in intestine tissue samples and rectal swabs of the vehicle source animals and their contacts but were undetectable in the MK-4482/EIDD-2801-treated source group and co-housed contact animals.

Phylogenetic analysis of outbreaks in mink farms revealed prolonged intra-colony circulation and zoonotic mink-to-human transmission[9], driving our selection of ferrets, members of the weasel genus closely related to minks, as a SARS-CoV-2 transmission model. We noted strong viral inoculum amount-dependence of experimental infection of ferrets. Productive host invasion was only observed after intranasal delivery of 100,000 pfu of SARS-CoV-2. Shed SARS-CoV-2 load in ferret nasal lavages, a core virological marker of a transmission model, showed good cross-study consistency. Our experiments returned peak shed virus titers of 10^3–10^4 pfu/ml, closely resembling ferret lavage titers found in two previous studies, which reported up to 10^4 pfu/ml[20] and up to 10^3 $TCID_{50}$/ml[21] in nasal lavages, respectively.

Natural infection through direct contact was highly efficient, possibly reflecting prolonged exposure of contact to source animals in a confined space. However, nearly all contacts started to shed virus within less than 24 hours after the beginning of co-housing. This timeline indicates that transmission must have occurred shortly after introducing contact to source animals, despite the fact that shed viral titers of source animals were only 10^3 pfu/ml nasal lavage in this disease period. Transmission of SARS-CoV-2 between ferrets through the air has recently been demonstrated[22]. Our results underscore that natural infection with SARS-CoV-2 through large droplets, aerosols, and/or fomites is highly productive.

MK-4482/EIDD-2801 is currently being tested in advanced multi-center clinical trials, which were launched after successful completion of phase 1 safety trials (i.e. NCT04392219). Although dose levels applied in these studies and human PK data have not yet been disclosed, Merck & Co. have released[23] that NHC blood levels were safely reached in humans that exceed antiviral concentrations against SARS-CoV-2 in primary human airway epithelia cultures (NHC EC_{90} approx. 0.5–1 μM[13]). Our PK profiles for MK-4482/EIDD-2801 revealed that NHC plasma concentrations ≥0.5 μM at trough (12 hours after dosing based on a *b.i.d.* regimen) are reached after oral dose levels of approximately 130 mg/kg and 10 mg/kg in cynomolgus macaques and ferrets, respectively[4]. These calculations drove our decision to dose ferrets at the 5 mg/kg level in this study, which represents a conservative estimate of a safe human dose equivalent based on all available information. Underscoring the high broad-spectrum antiviral potential of the drug, 5 mg/kg is also close to the lowest efficacious dose of MK-4482/EIDD-2801 against seasonal and pandemic influenza viruses in ferrets[4,10].

Closely resembling our prior experience with influenza therapy[4,10], MK-4482/EIDD-2801 was well tolerated and orally efficacious against SARS-CoV-2, reducing upper respiratory virus load below detection level within 24 hours of first drug administration when therapy

was initiated after the onset of virus shedding, and by nearly two orders of magnitude when first administered at the peak of virus replication. Viral genetic material in gastrointestinal samples was likewise undetectable in treated animals, which is consistent with previous observations of sustained presence of the biologically active triphosphate form of NHC in all soft tissue but liver in different species[4,12,24].

Importantly, treatment suppressed all transmission to untreated direct contacts, despite prolonged direct proximity of source and contact animals and detectable virus shedding from source animals at the beginning of the co-housing phase. This complete block may indicate a bottom threshold of shed SARS-CoV-2 load for successful spread. In addition, genome integrity of some EIDD-2801-experienced virions shed from treated animals may have been only partially compromised. Rather than being chain-terminating when incorporated by the viral polymerase, NHC undergoes spontaneous tautomeric interconversions, leading to base pairing either as cytosine or uracil[25]. The resulting randomly positioned transition mutations induce viral error catastrophe[26], causing collapse of the virus population. This mechanism of antiviral activity of NHC was demonstrated for alphaviruses[12], pneumoviruses[11], orthomyxoviruses[4], and confirmed to equally apply to betacoronaviruses[19] and SARS-CoVs, specifically[13]. In our study, limited presence of the analogue in viral genomes generated shortly after treatment start may have had a greater impact on natural invasion of an immune-competent host *in vivo* than on virus replication in type I interferon-deficient cultured cells such as the Vero E6 used for titration[27]. This view is consistent with the frequent observation (i.e.[28]) that many mutant viruses can be propagated in cell culture but are attenuated *in vivo* and incapable of productive host invasion.

Consistent with the conserved antiviral mechanism of action of NHC across diverse viral targets, extensive previous attempts to induce robust resistance to the compound in alphaviruses[12], orthomyxoviruses[4], and betacoronaviruses[19] were unsuccessful, indicating a high genetic barrier against viral escape. For betacoronaviruses specifically, a very moderate 2-fold increase in EC_{90} concentration was reported after 30 passages in the presence of inhibitor[19]. Since these mutations delayed viral replication and thus posed a fitness penalty, it is unlikely that clinical use of MK-4482/EIDD-2801 will result in the emergence of preexisting resistance in circulating virus populations or trigger the appearance of viral variants with enhanced pathogenicity.

Our prior studies with influenza viruses in ferrets[4] and guinea pigs[11] furthermore demonstrated that antiviral efficacy and transmission block by MK-4482/EIDD-2801 are not host species-restricted. A virological study of hospitalized patients with COVID-19 has revealed that the average load of SARS-CoV-2 RNA copies detected in human sputum during the peak phase of infection was 7.0×10^6 (maximum 2.35×10^9) copies/ml[29]. Virus isolation attempts from human patients were in general unsuccessful when samples contained $<10^6$ RNA copies per ml. In ferrets, we found peak shedding titers of 10^3–10^4 pfu/ml in nasal lavages and an earlier study reported that up to 10^4 pfu of SARS-CoV-2 per ml of ferret nasal lavage approximately correlate to up to 10^8 viral RNA copies/ml[20]. These comparisons suggest that peak viral RNA copy load in ferret nasal lavages recapitulates that seen in human sputum. At present, tissue distribution and antiviral efficacy of MK-4482/EIDD-2801 in humans are still unknown. If ferret-based inhibition data of SARS-CoV-2

transmission are predictive of the effect in humans, however, COVID-19 patients could become non-infectious within 24 to 36 hours after the onset of oral treatment. Treatment with MK-4482/EIDD-2801, in particular when initiated early after infection, thus has the potential to provide three-fold benefit: it may mitigate the risk of progression to severe disease and accelerate recovery, ease the emotional and socioeconomic toll associated with mandatory prolonged isolation, and aid in rapidly silencing local outbreaks.

Methods

Study design

Ferrets were used as an *in vivo* model to examine efficacy of therapeutically administered oral MK-4482/EIDD-2801 against SARS-CoV-2 infection and virus transmission to uninfected contact animals. Viruses were administered to source animals through intranasal inoculation and virus load monitored periodically in nasal lavages and rectal swabs, and 4 or 10 days after exposure in respiratory tissues and a subset of organs. Virus titers were determined based on plaque assay and viral RNA copy numbers, blood samples subjected to CBC analysis and RT-qPCR quantitation of selected cytokine and innate antiviral effector expression levels.

Cells and viruses

Vero E6 cells were obtained from ATCC (ATCC CRLK-1586) and cultured in Dulbecco's modified Eagle's medium (DMEM) supplemented with 7.5% heat inactivated fetal bovine serum (FBS) at 37°C with 5% CO_2. SARS-CoV-2 (SARS-CoV-2/human/USA-WA1/2020) was propagated using Vero E6 cells supplemented with 2% FBS. Virus stocks were stored at −80°C and titers were determined by plaque assay. Vero E6 cells were authenticated by morphology and susceptibility to virus infection, and routinely checked in 6-month intervals for bacterial and mycoplasma contamination.

Virus yield reduction assay

Vero E6 cells were seeded in 12-well plates at 3×10^5 cells per well 24-hours prior to infection. Cells were infected using a multiplicity of infection (MOI) of 0.1 pfu per cell. SARS-CoV-2 was allowed to adsorb for one hour at 37°C. Subsequently, virus inoculum was removed and cells were overlaid with media containing 3-fold serial dilutions of NHC (50–0.68 μM) in DMEM supplemented with 2% FBS. Infected cells were incubated with compound for 48 hours at 37°C, followed by virus titration by plaque assay. EC_{50} and EC_{90} concentrations were calculated using four-parameter variable-slope regression modeling.

Plaque assay

Samples were serially diluted (10-fold starting at 1:10 initial dilution) in DMEM supplemented with 2% FBS containing antibiotics-antimycotics (Gibco). Serial dilutions were added to Vero E6 cells seeded in 12-well plates at 3×10^5 cells per well 24-hours prior. Virus was allowed to adsorb for 1 hour at 37°C. Subsequently, inoculum was removed, and cells were overlaid with 1.2% Avicel (FMC biopolymer) in DMEM and incubated for three days at 37°C with 5% CO_2. Avicel was removed and cells were washed once with PBS,

fixed with 10% neutral buffered formalin, and plaques were visualized using 1% crystal violet.

Establishing infectious dose

Female ferrets (6–10 months of age) were purchased from Triple F Farms. Upon arrival, ferrets were rested for one week, then randomly assigned to groups and housed individually in ventilated negative pressure cages in an ABSL-3 facility. In order to establish a suitable inoculum for efficacy and transmission studies, ferrets (n=4) were inoculated intranasally with 1×10^4 and 1×10^5 pfu of 2019-nCoV/USA-WA1/2020 in 1 ml (0.5 ml per nare). Prior to inoculation, ferrets were anesthetized with dexmedetomidine/ketamine. Nasal lavages were performed once daily on non-anesthetized animals using 1 ml of PBS containing 2-fold concentrated antibiotics-antimycotics (Gibco). Nasal lavage fluids were stored at −80°C until virus titration through plaque assays on Vero E6 cells. For blood sampling, ferrets were anesthetized with dexmedetomidine and approximately 0.5 ml blood was drawn from the anterior vena cava. Complete blood counts (CBC) were performed using a Vetscan HM5 (Abaxis) in accordance with the manufacturer's protocol. Rectal swabs were performed every two days. Groups of two ferrets were sacrificed 4- and 10-days post infection and organs were harvested to determine virus titer and the presence of viral RNA in different tissues.

Animals

Group sizes in all animal experiments were three ferrets (Mustela putorius furo) per condition. Power calculation ($P<0.05$; 80% power) predicted that this sample size will detect a difference of 1.19 log10 pfu/ml in virus titer in ferret nasal lavages. Since no statistically informative reference data sets for the SARS-CoV-2 ferret model were available at study start, we based this prospective calculation on our experience with a canine distemper virus ferret infection model, which has shown a cumulative SD of 0.32 in our laboratory. In transmission experiments, ferrets were co-housed at a ratio of one source to two contact animals, three co-housing sets per condition. Incoming animals were assigned to the different study groups randomly; no blinding of investigators was performed.

In vivo efficacy of MK-4482/EIDD-2801 in ferrets

Groups of ferrets were inoculated with 1×10^5 pfu of 2019-nCoV/USA-WA1/2020 in 1 ml (0.5 ml per nare). At 12 hours after infection, three groups of ferrets were treated *b.i.d.* with vehicle (1% methylcellulose) or MK-4482/EIDD-2801 at a dose level of 5 mg/kg or 15 mg/kg, respectively. At 36 hours after infection, a fourth group of ferrets began receiving *b.i.d.* treatment with MK-4482/EIDD-2801 at a dose of 15 mg/kg. Compound was administered via oral gavage in 1% methylcellulose. After treatment onset, *b.i.d.* dosing was continued until four days after infection. Nasal lavages were performed on all ferrets every 12 hours. Blood samples were obtained every two days after infection and stored in K_2-EDTA tubes (Sarstedt CB 300). CBC analysis was performed on each blood sample in accordance with the manufacturer's protocols. After CBC analysis, red blood cells were lysed with ACK buffer (150 mM NH_4CL, 10mM $KHCO_3$, 0.01 mM EDTA pH 7.4) and PBMCs were harvested and stored at −80°C in RNAlater until further qPCR analysis was

performed. Four days after infection, all ferrets were euthanized and organs harvested to determine virus titers and the presence of viral RNA in different tissues.

Contact transmission of SARS-CoV-2 in ferrets

A group of 6 individually housed source ferrets were inoculated intranasally with 1×10^5 pfu of 2019-nCoV/USA-WA1/2020. Twelve hours after infection, source ferrets were split into two groups (n=3 each) receiving vehicle or MK-4482/EIDD-2801 treatment at a dose of 5 mg/kg *b.i.d.* daily by oral gavage. At 30 hours post infection, each source ferret was co-housed with two uninfected and untreated contact ferrets. Ferrets were co-housed until 96 hours after infection, when source ferrets were euthanized and contact animals housed individually. Contact animals were monitored for four days after separation from source ferrets, then sacrificed. Nasal lavages and rectal swabs were performed every 24 hours on all ferrets. Blood samples were collected at 0, 4, and 8 days after source ferret infection. For all ferrets, organs were harvested to determine virus titers and the presence of viral RNA in different tissues.

Titration of SARS-CoV-2 in tissue extracts

For virus titration, organs were weighed and homogenized in PBS. Homogenates were centrifuged for 5 minutes at 2,000×g at 4°C. Clarified supernatants were harvested and used in subsequent plaque assays. For detection of viral RNA, harvested organs were stored in RNAlater at −80°C. Tissues were ground and total RNA was extracted using a RNeasy mini kit (Qiagen). RNA was extracted from rectal swabs using the ZR Viral RNA Kit (Zymo Research) in accordance with the manufacturer's protocols.

SARS-CoV-2 RNA copy numbers

Detection of SARS-CoV-2 RNA was performed using the nCoV_IP2 primer-probe set (National Reference Center for Respiratory Viruses, Institut Pasteur, Paris) targeting the SARS-CoV-2 RdRp gene. An Applied Biosystems 7500 Real-Time PCR System using the StepOnePlus Real-Time PCR System was used to perform qPCR reactions. TaqMan Fast Virus 1-Step Master Mix (Thermo Fisher Scientific) was used in combination with the nCoV_IP2 primer-probe set to detect viral RNA. To quantitate RNA copy numbers, a standard curve was created using a PCR fragment (nucleotides 12669–14146 of the SARS-CoV-2 genome) generated from viral cDNA using nCoV_IP2 forward primer and the nCoV_IP4 reverse primer. RNA values were normalized based on weights of tissues used.

Systemic interferon and cytokine profiling

Relative expression of interferon, interferon stimulated genes and cytokines was determined by real-time PCR analyses. RNA was extracted from PBMCs harvested at various times after infection. cDNA was reverse transcribed with SuperScript III (Invitrogen) using oligo-dT primers and analyzed by real-time PCR using Fast SYBR Green Master Mix (Applied Biosystems). Signals were normalized to glyceraldehyde-3-phosphate dehydrogenase mRNA, analyzed by the comparative threshold cycle (ΔΔCt) method, and expressed relative to day 0 of infection for each respective animal. Sequences of the primers used for the analyses are shown in Supplementary Table 13.

Statistics and Reproducibility

Microsoft Excel (versions 16.42 and 16.43) and GraphPad Prism (version 8.4.3) software packages were used for most data collection and analysis, respectively. Reverse transcription qPCR data was collected and analyzed using the StepOnePlus (Version 2.1; Applied Biosystems) software package. Final figures were assembled using Adobe Illustrator (version CS6). One-way or two-way analysis of variance (ANOVA) with Dunnett's, Tukey's, or Sidak's multiple comparisons post-hoc tests without further adjustments were used to evaluate statistical significance when more than two groups were compared or datasets contained two independent variables, respectively. The specific statistical test applied to individual studies is specified in figure legends. Source Data files summarize the statistical analyses (effect size, degrees of freedom, P values) for the respective datasets. Effect sizes between groups in ANOVAs were calculated as $\eta^2 = (SS_{effect}) / (SS_{total})$ [one-way ANOVA] and $\omega^2 = (SS_{effect} - (df_{effect})(MS_{error})) / MS_{error} + SS_{total}$ [two-way ANOVA]. To determine antiviral potency and cytotoxicity, effective concentrations were calculated from dose-response data sets through 4-parameter variable slope regression modeling; values are expressed with 95% confidence intervals (CIs) when possible. Biological repeat refers to measurements taken from distinct samples, and results obtained for each individual biological repeat are shown in the figures along with the exact size (n number) of biologically independent samples, animals, or independent experiments. Measure of center (connecting lines and columns) are means throughout. Error bars represent standard deviations (SD) throughout. For all experiments, the statistical significance level α was set to <0.05, exact P values are shown in individual graphs or Supplement Tables wherever possible.

Extended Data

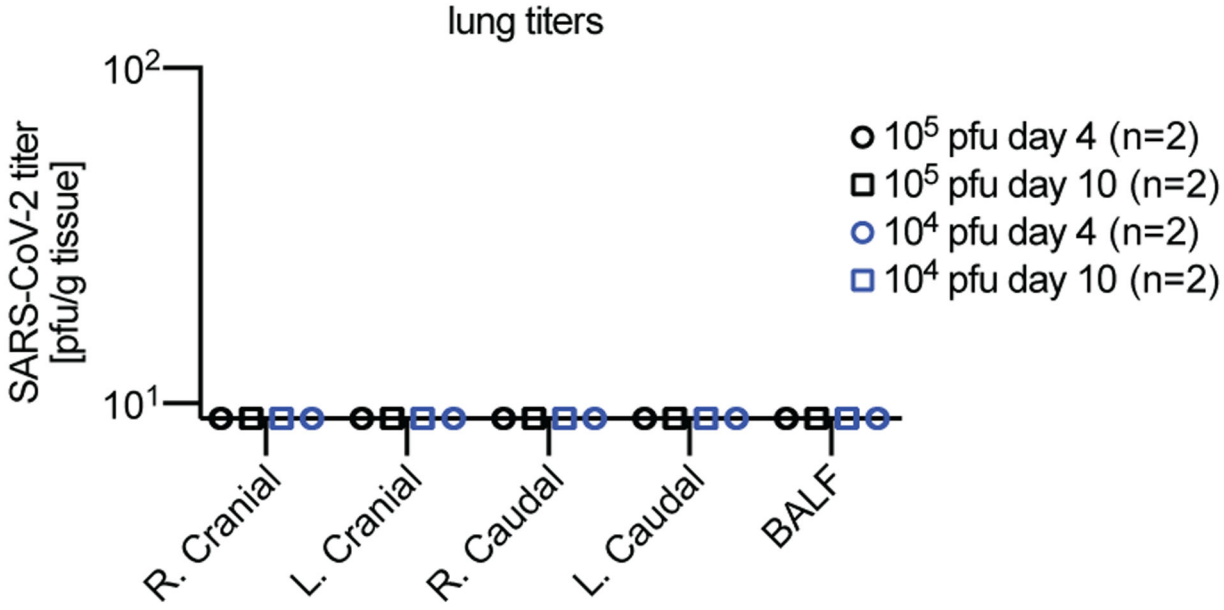

Extended Data Fig. 1. SARS-CoV-2 does not progress to the ferret lower respiratory tract.

Ferrets were inoculated intranasally with 1×10^4 (blue) or 1×10^5 pfu (black) of 2019-nCoV/USA-WA1/2020. **a,** Analysis of bronchioalveolar lavages (BALF) and four lung lobes (right (R.) and left (L.) cranial and caudal) per ferret. BALF and tissues samples were harvested 4 (n=2 biologically independent animals) and 10 (n=2 biologically independent animals) days after infection. The number of independent biological repeats is shown. Symbols represent independent biological repeats (individual animals).

Extended Data 2a | Comparison of SARS-CoV-2 titers in nasal lavages of SARS-CoV-2 infected ferrets treated with different doses and dosing regimens

				intergroup comparison: 5 mg/kg 12 hpi	
group	days pI	mean titer [pfu/ml]	SD [pfu/ml]	vs 15 mg/kg 12 hpi[A] (P value)	vs 15 mg/kg 36 hpi (P value)
vehicle	0	<LoD	n.a.[B]	--	--
	0.5	5.33×10^2	4.93×10^2	--	--
	1	1.60×10^3	6.56×10^2	--	--
	1.5	1.33×10^3	5.77×10^2	--	--
	2	1.40×10^3	5.29×10^2	--	--
	2.5	3.33×10^2	3.21×10^2	--	--
	3	4.67×10^2	1.15×10^2	--	--
	3.5	6.33×10^1	3.21×10^1	--	--
5 mg/kg 12 hpi	0	<LoD	n.a.	--	--
	0.5	6.40×10^1	5.15×10^2	NS; 0.9982	NS; 0.9816
	1	8.67×10^1	4.51×10^1	NS; 0.997	NS; 0.068
	1.5	<LoD	n.a.	NS; 0.7106**	NS; 0.0669**
	2	<LoD	n.a.	NS; 0.7683**	0.0107**
	2.5	<LoD	n.a.	--	NS; 0.4711**
	3	<LoD	n.a.	--	--
	3.5	<LoD	n.a.	--	--
15 mg/kg 12 hpi	0	<LoD	n.a.	--	--
	0.5	5.53×10^2	5.64×10^2	--	NS; 0.9966
	1	9.00×10^1	6.08×10^1	--	NS; 0.1143
	1.5	16.33*	n.a.	--	NS; 0.053*
	2	12.67*	n.a.	--	0.0028*
	2.5	<LoD	n.a.	--	NS; 0.4711**
	3	<LoD	n.a.	--	--
	3.5	<LoD	n.a.	--	--
15 mg/kg 36 hpi	0	<LoD	n.a.	--	--
	0.5	4.33×10^2	4.04×10^2	--	--
	1	9.67×10^2	5.86×10^2	--	--
	1.5	2.10×10^3	2.54×10^1	--	--
	2	3.33×10^2	1.15×10^2	--	--
	2.5	23*	15.7	--	--
	3	<LoD	n.a.	--	--
	3.5	<LoD	n.a.	--	--

[A]hpI; hours post infection
[B]n.a.; not applicable

Extended Data 2b | SARS-CoV-2 titers in nasal turbinates of ferrets

				intergroup comparison: 5 mg/kg 12 hpi	
group	days pI	mean titer [pfu/ml]	std dev. [pfu/ml]	vs 15mg/kg 12hpi (P value)	vs 15 mg/kg 36 hpi (P value)
vehicle	4	2.81×10^3	3.28×10^3	--	--
5 mg/kg 12 hpi	4	<L.o.D	n.a.	NS; >0.9999**	NS; >0.9999**
15 mg/kg 12 hpi	4	<L.o.D	n.a.	--	NS; >0.9999**
15 mg/kg 36 hpi	4	<L.o.D	n.a.	--	--

Extended Data 2c | Viral RNA detected in nasal turbinates of ferrets

				intergroup comparison: 5 mg/kg 12 hpi	
group	days pI	mean RNA [copies/g tissue]	std dev. [copies/g tissue]	vs 15mg/kg 12hpi (P value)	vs 15 mg/kg 36 hpi (P value)
vehicle	4	1.13×10^6	6.24×10^5	--	--
5 mg/kg 12 hpi	4	1.16×10^5	7.10×10^4	NS; 0.9998	0.042
15 mg/kg 12 hpi	4	1.06×10^5	5.15×10^4	--	0.0378
15 mg/kg 36 hpi	4	8.64×10^5	6.25×10^5	--	--

Extended Data Fig. 2. Experimental means and intergroup comparison of *in vivo* efficacy study results of MK-4482/EIDD-2801 in SARS-CoV-2-infected ferrets.

a, Comparison of SARS-CoV-2 titers in nasal lavages of SARS-CoV-2 infected ferrets treated with different doses and dosing regimens. Mean virus titers ± SD are shown for different study days (days pI). The limit of detection (LoD) was 10 pfu (a-b). Samples below

LoD were plotted as 9 pfu. **b**, SARS-CoV-2 titers in nasal turbinates of ferrets from (a). Mean virus titers ± SD are shown. LoD was 10 pfu (a-b). **c,** Viral RNA detected in nasal turbinates of ferrets from (a). Mean RNA copy numbers ± SD are shown. Statistical significance was determined between different treatment groups. LoD was 1 RNA copy, samples below LoD were plotted as 1 RNA copy. Statistical analysis was performed by two-way (a) or one-way (b-c) ANOVA with Tukey's multiple comparison post-hoc test. P values are shown. (*) denotes samples where one or two repeats were below LoD. (**) denotes all three repeats for at least one dosing group were below LoD.

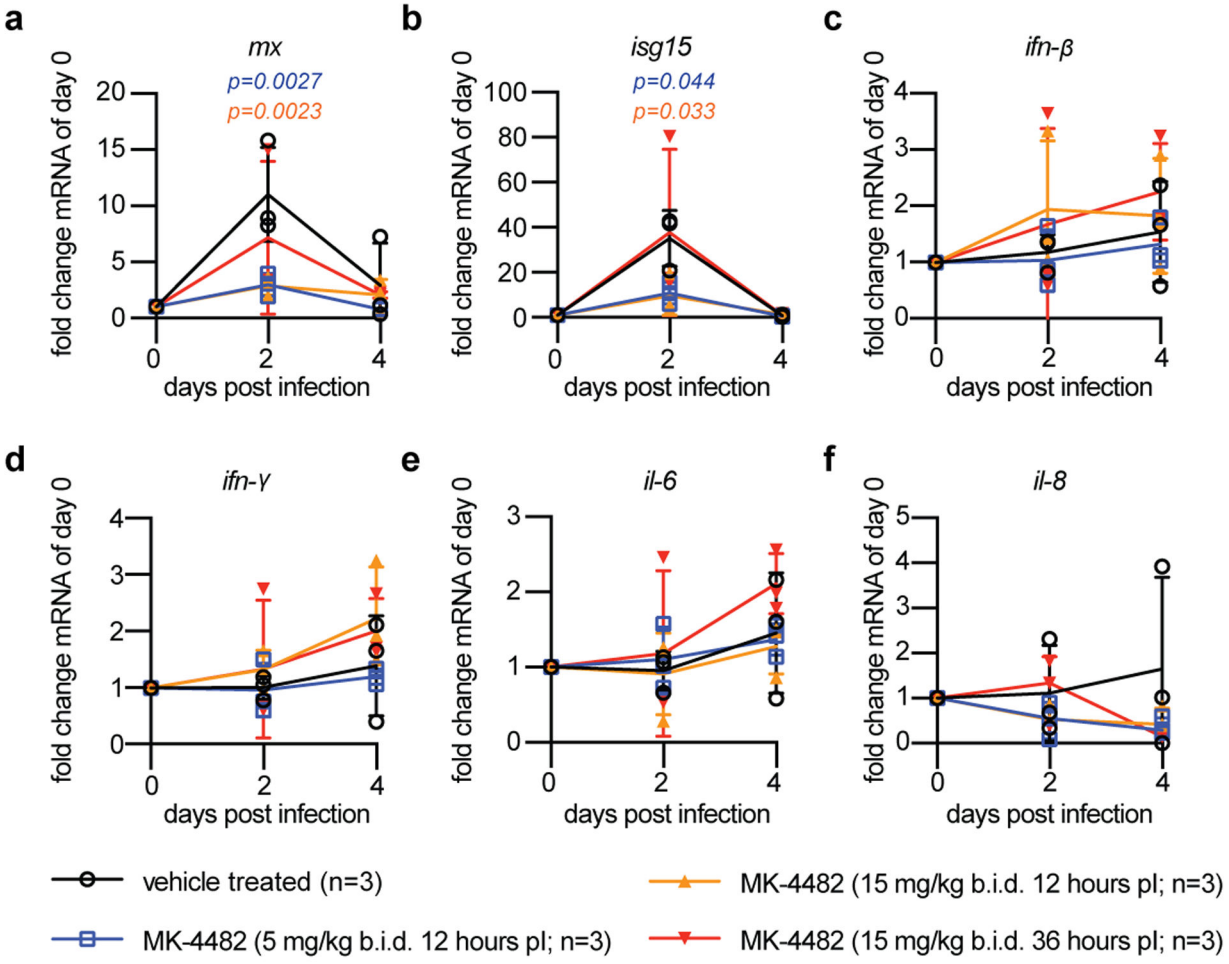

Extended Data Fig. 3. Interferon induction and cytokine profiling of SARS-CoV-2 ferrets treated with MK-4482/EIDD-2801.

Ferrets (n=3 biologically independent animals) were infected intranasally with 1×10^5 pfu 2019-nCoV/USA-WA1/2020 and either gavaged with vehicle (black (a-f)) or treated *b.i.d.* with MK-4482/EIDD-2801 commencing 12 (5 mg/kg (blue (a-f)) and 15 mg/kg (orange (a-f)) or 36-hours (15 mg/kg; red (a-f)) after infection. **a-f,** Selected interferon and cytokine expression levels in PBMCs relative to day 0. Blood samples of animals treated with MK-4482/EIDD-2801 or vehicle as specified were collected every two days after infection and PBMCs analyzed by RT-qPCR. Statistical analysis of changes relative to day 0 by two-way ANOVA with Dunnett's post-hoc multiple comparison test. The number of independent

biological repeats (n; individual animals) is shown. In all panels, symbols represent independent biological repeats (individual animals), lines connect group means ± SD.

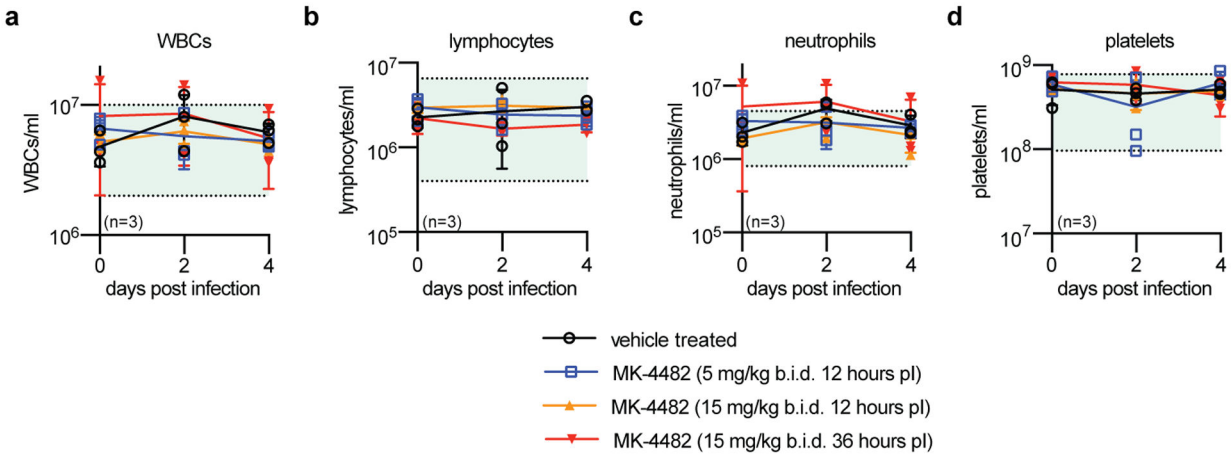

Extended Data Fig. 4. Complete blood count of SARS-CoV-2 ferrets treated with MK-4482/EIDD-2801.

Ferrets (n=3 biologically independent animals) were infected intranasally with 1×10^5 pfu 2019-nCoV/USA-WA1/2020 and either gavaged with vehicle (black (a-f)) or treated *b.i.d.* with MK-4482/EIDD-2801 commencing 12 (5 mg/kg (blue (a-f)) and 15 mg/kg (orange (a-f)) or 36-hours (15 mg/kg; red (a-f)) after infection. **a-d**, Blood samples were collected every two days after infection and complete blood counts determined. No abnormal values were observed in all parameters tested, including total WBCs (a), lymphocytes (b), neutrophils (c), and platelets (d). The shaded green areas represent normal Vetscan HM5 lab values. The number of independent biological repeats (n; individual animals) is shown for each subpanel. Symbols represent independent biological repeats (individual animals), lines connect group means ± SD.

Supplementary Material

Refer to Web version on PubMed Central for supplementary material.

Acknowledgements

We thank M. Kumar for providing an aliquot of 2019-nCoV/USA-WA1/2020 stock, members of the GSU High Containment Core and the Department for Animal Research for support, and J. Sourimant and A. L. Hammond for critical reading of the manuscript. This work was supported, in part, by Public Health Service grants AI071002 (to RKP) and AI141222 (to RKP), from the NIH/NIAID. The funders had no role in study design, data collection and interpretation, or the decision to submit the work for publication.

References

1. Rodriguez Mega E COVID has killed more than one million people. How many more will die? Nature, doi:10.1038/d41586-020-02762-y (2020).
2. Martinot M et al. Remdesivir failure with SARS-CoV-2 RNA-dependent RNA-polymerase mutation in a B-cell immunodeficient patient with protracted Covid-19. Clin. Infect. Dis, doi:10.1093/cid/ciaa1474 (2020).

3. Humeniuk R et al. Safety, Tolerability, and Pharmacokinetics of Remdesivir, An Antiviral for Treatment of COVID-19, in Healthy Subjects. Clin. Transl. Sci 13, 896–906, doi:10.1111/cts.12840 (2020). [PubMed: 32589775]
4. Toots M et al. Characterization of orally efficacious influenza drug with high resistance barrier in ferrets and human airway epithelia. Sci. Transl. Med 11, doi:10.1126/scitranslmed.aax5866 (2019).
5. Toots M & Plemper RK Next-generation direct-acting influenza therapeutics. Transl. Res, doi:10.1016/j.trsl.2020.01.005 (2020).
6. Salajegheh Tazerji S et al. Transmission of severe acute respiratory syndrome coronavirus 2 (SARS-CoV-2) to animals: an updated review. J. Transl. Med 18, 358, doi:10.1186/s12967-020-02534-2 (2020). [PubMed: 32957995]
7. Oreshkova N et al. SARS-CoV-2 infection in farmed minks, the Netherlands, April and May 2020. Euro Surveill. 25, doi:10.2807/1560-7917.ES.2020.25.23.2001005 (2020).
8. Enserink M Coronavirus rips through Dutch mink farms, triggering culls. Science 368, 1169, doi:10.1126/science.368.6496.1169 (2020). [PubMed: 32527808]
9. Oude Munnink BB et al. Jumping back and forth: anthropozoonotic and zoonotic transmission of SARS-CoV-2 on mink farms. bioRxiv, 2020.2009.2001.277152, doi:10.1101/2020.09.01.277152 (2020).
10. Toots M et al. Quantitative efficacy paradigms of the influenza clinical drug candidate EIDD-2801 in the ferret model. Transl. Res 218, 16–28, doi:10.1016/j.trsl.2019.12.002 (2020). [PubMed: 31945316]
11. Yoon JJ et al. Orally Efficacious Broad-Spectrum Ribonucleoside Analog Inhibitor of Influenza and Respiratory Syncytial Viruses. Antimicrob. Agents Chemother 62, doi:10.1128/AAC.00766-18 (2018).
12. Urakova N et al. beta-d-N (4)-Hydroxycytidine Is a Potent Anti-alphavirus Compound That Induces a High Level of Mutations in the Viral Genome. J. Virol 92, doi:10.1128/JVI.01965-17 (2018).
13. Sheahan TP et al. An orally bioavailable broad-spectrum antiviral inhibits SARS-CoV-2 in human airway epithelial cell cultures and multiple coronaviruses in mice. Sci. Transl. Med 12, doi:10.1126/scitranslmed.abb5883 (2020).
14. Han K et al. Lung Expression of Human ACE2 Sensitizes the Mouse to SARS-CoV-2 Infection. Am. J. Respir. Cell Mol. Biol, doi:10.1165/rcmb.2020-0354OC (2020).
15. Bruschke C (ed Nature and Food Quality Ministry of Agriculture) (2020).
16. Schlottau K et al. SARS-CoV-2 in fruit bats, ferrets, pigs, and chickens: an experimental transmission study. Lancet Microbe 1, e218–e225, doi:10.1016/S2666-5247(20)30089-6 (2020). [PubMed: 32838346]
17. Richard M et al. SARS-CoV-2 is transmitted via contact and via the air between ferrets. Nat Commun 11, 3496, doi:10.1038/s41467-020-17367-2 (2020). [PubMed: 32641684]
18. Davies NG et al. Age-dependent effects in the transmission and control of COVID-19 epidemics. Nat. Med 26, 1205–1211, doi:10.1038/s41591-020-0962-9 (2020). [PubMed: 32546824]
19. Agostini ML et al. Small-Molecule Antiviral beta-d-N (4)-Hydroxycytidine Inhibits a Proofreading-Intact Coronavirus with a High Genetic Barrier to Resistance. J. Virol 93, doi:10.1128/JVI.01348-19 (2019).
20. Shi J et al. Susceptibility of ferrets, cats, dogs, and other domesticated animals to SARS-coronavirus 2. Science 368, 1016–1020, doi:10.1126/science.abb7015 (2020). [PubMed: 32269068]
21. Park SJ et al. Antiviral Efficacies of FDA-Approved Drugs against SARS-CoV-2 Infection in Ferrets. mBio 11, doi:10.1128/mBio.01114-20 (2020).
22. Kutter JS et al. SARS-CoV and SARS-CoV-2 are transmitted through the air between ferrets over more than one meter distance. bioRxiv, 2020.2010.2019.345363, doi:10.1101/2020.10.19.345363 (2020).
23. in GEN Genetic Engineering & Biotechnology News (2020).
24. Painter GR et al. The prophylactic and therapeutic activity of a broadly active ribonucleoside analog in a murine model of intranasal venezuelan equine encephalitis virus infection. Antiviral Res. 171, 104597, doi:10.1016/j.antiviral.2019.104597 (2019). [PubMed: 31494195]

25. Les A, Adamowicz L & Rode W Structure and conformation of N4-hydroxycytosine and N4-hydroxy-5-fluorocytosine. A theoretical ab initio study. Biochim. Biophys. Acta 1173, 39–48, doi:10.1016/0167-4781(93)90240-e (1993). [PubMed: 8485152]

26. Crotty S, Cameron CE & Andino R RNA virus error catastrophe: direct molecular test by using ribavirin. Proc. Natl. Acad. Sci. U. S. A 98, 6895–6900, doi:10.1073/pnas.111085598 (2001). [PubMed: 11371613]

27. Desmyter J, Melnick JL & Rawls WE Defectiveness of interferon production and of rubella virus interference in a line of African green monkey kidney cells (Vero). J. Virol 2, 955–961, doi:10.1128/JVI.2.10.955-961.1968 (1968). [PubMed: 4302013]

28. Cox RM et al. Orally efficacious broad-spectrum allosteric inhibitor of paramyxovirus polymerase. Nat Microbiol, doi:10.1038/s41564-020-0752-7 (2020).

29. Wolfel R et al. Virological assessment of hospitalized patients with COVID-2019. Nature 581, 465–469, doi:10.1038/s41586-020-2196-x (2020). [PubMed: 32235945]

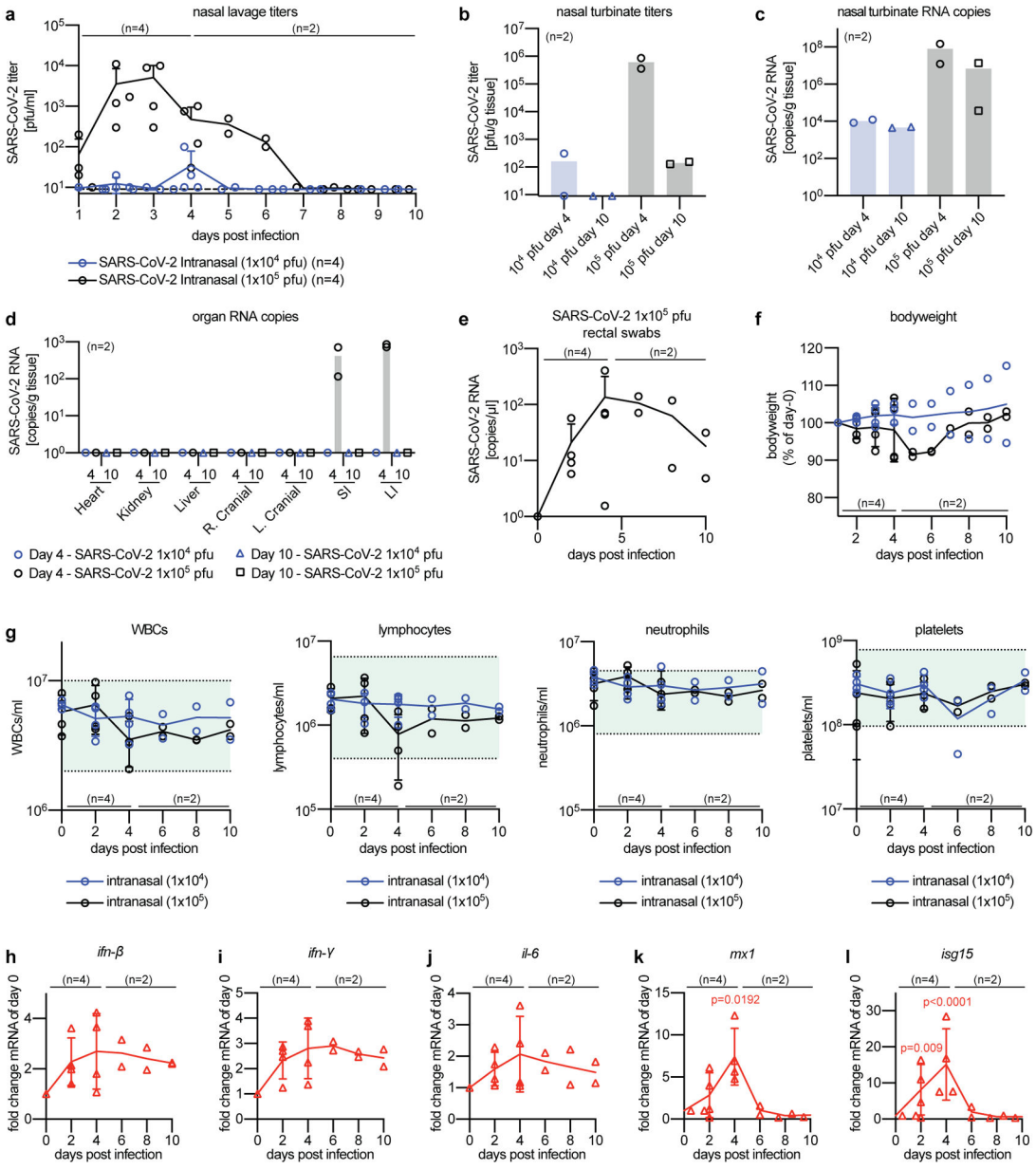

Fig. 1.

SARS-CoV-2 infects the upper respiratory tract of ferrets. Ferrets (n=4 biologically independent animals) were inoculated intranasally with 1×10^4 (blue throughout) or 1×10^5 pfu (black throughout) of 2019-nCoV/USA-WA1/2020. **a**, Virus titer in nasal lavages collected daily. **b-f**, At 4 and 10 days post infection, 2 ferrets were sacrificed in each group and infection was characterized. **b,** Infectious virus particles in nasal turbinates. **c,** Viral RNA was present in the nasal turbinates of all infected ferrets. **d**, RT-qPCR quantitation of viral RNA copies in selected organs, two lung lobes (right (R.) and left (L.) cranial) per animal, and small (SI) and large (LI) intestine samples extracted from infected ferrets four or 10 days after infection. **e,** Detection of 2019-nCoV/USA-WA1/2020 RNA in rectal swabs of ferrets inoculated with 1×10^5 pfu. RNA was extracted from rectal swabs and absolute copy

numbers were determined by RT-qPCR. **f**, Bodyweight of ferrets, measured daily and expressed as % of weight at day 0. **g**, Complete blood count analysis, performed every second day. No noticeable differences were detected for all parameters tested, including total WBCs, lymphocytes, neutrophils, and platelets. The shaded green areas represent normal Vetscan HM5 lab values. **h-l**, Selected interferon and cytokine responses in PBMCs harvested every two days after infection. Analysis by qPCR for animals infected with 1×10^5 pfu of 2019-nCoV/USA-WA1/2020. Infected ferrets displayed elevated expression of *ifn-β* (h) and *ifn-γ* (i). *il-6* was moderately elevated only in some animals (j). Interferon stimulated genes (*mx1* (k; p=0.0192 on day 4) and *isg15* (l; p=0.009 and p<0.0001 on days 2 and 4, respectively)) showed a sharp peak at day 4 after infection. The number of independent biological repeats (n; individual animals) is shown for each subpanel. Statistical analysis by two-way ANOVA with Dunnett's post-hoc multiple comparison test. In all panels, symbols represent independent biological repeats (individual animals), lines connect group means ± SD (a,e-l), and bar graphs show means only (b-d).

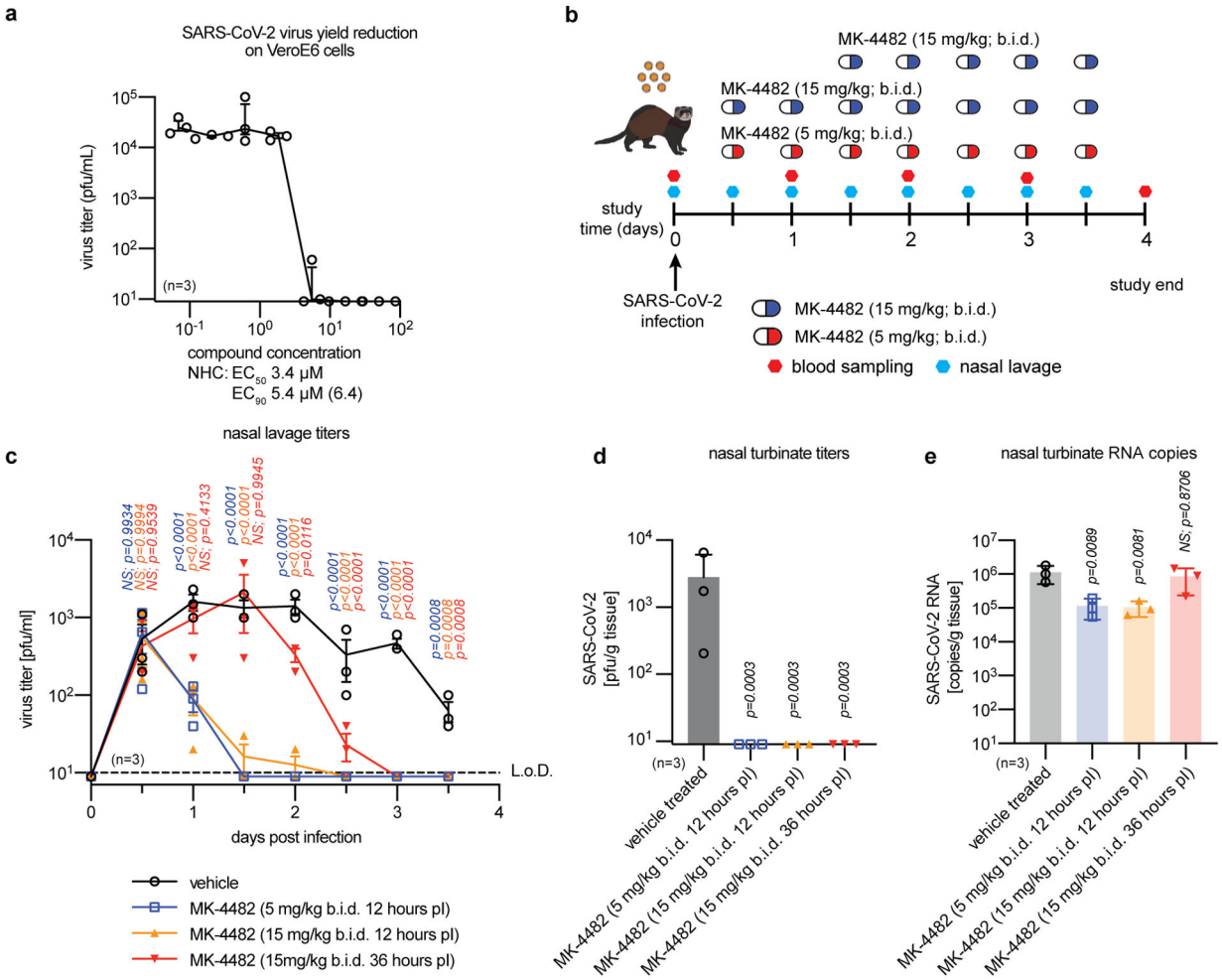

Fig. 2.

Therapeutic MK-4482/EIDD-2801 is orally efficacious against SARS-CoV-2 in ferrets. **a,** Dose-response inhibition test of NHC against SARS-CoV-2 in Vero E6 cells (MOI 0.1 pfu/cell; n=3 biologically independent experiments). Effective concentrations (EC_{50} and EC_{90}, shown with upper 95% confidence interval limit in parenthesis) are derived from four-parameter variable slope regression modeling. **b,** Therapeutic efficacy study schematic. Ferrets (n=3 biologically independent animals) were infected intranasally with 1×10^5 pfu 2019-nCoV/USA-WA1/2020 and either gavaged with vehicle (black (c-e)) or treated *b.i.d.* with MK-4482/EIDD-2801 commencing 12 (5 mg/kg (blue (c-e)) and 15 mg/kg (orange (c-e)) or 36-hours (15 mg/kg; red (c-e)) after infection. Nasal lavages were collected twice daily. Blood was collected every other day. **c**, Viral nasal lavage titers in infected ferrets from (a). Treatment with MK-4482/EIDD-2801 significantly reduced virus titers within 12 hours dosing onset in all treatment groups. Statistical analysis by two-way ANOVA with Dunnett's multiple comparison post-hoc test. P values are shown. **d-e,** Quantitation of infectious particles (d) and virus RNA copy numbers (e) in nasal turbinates of infected ferrets extracted four days after infection. Statistical analysis by one-way ANOVA with Dunnett's multiple comparison post-hoc test. The number of independent biological repeats is shown for each subpanel. P values are shown. In all panels, symbols represent

independent biological repeats (individual animals), lines connect group means ± SD (a,c) and bar graphs show means ± SD (d-e).

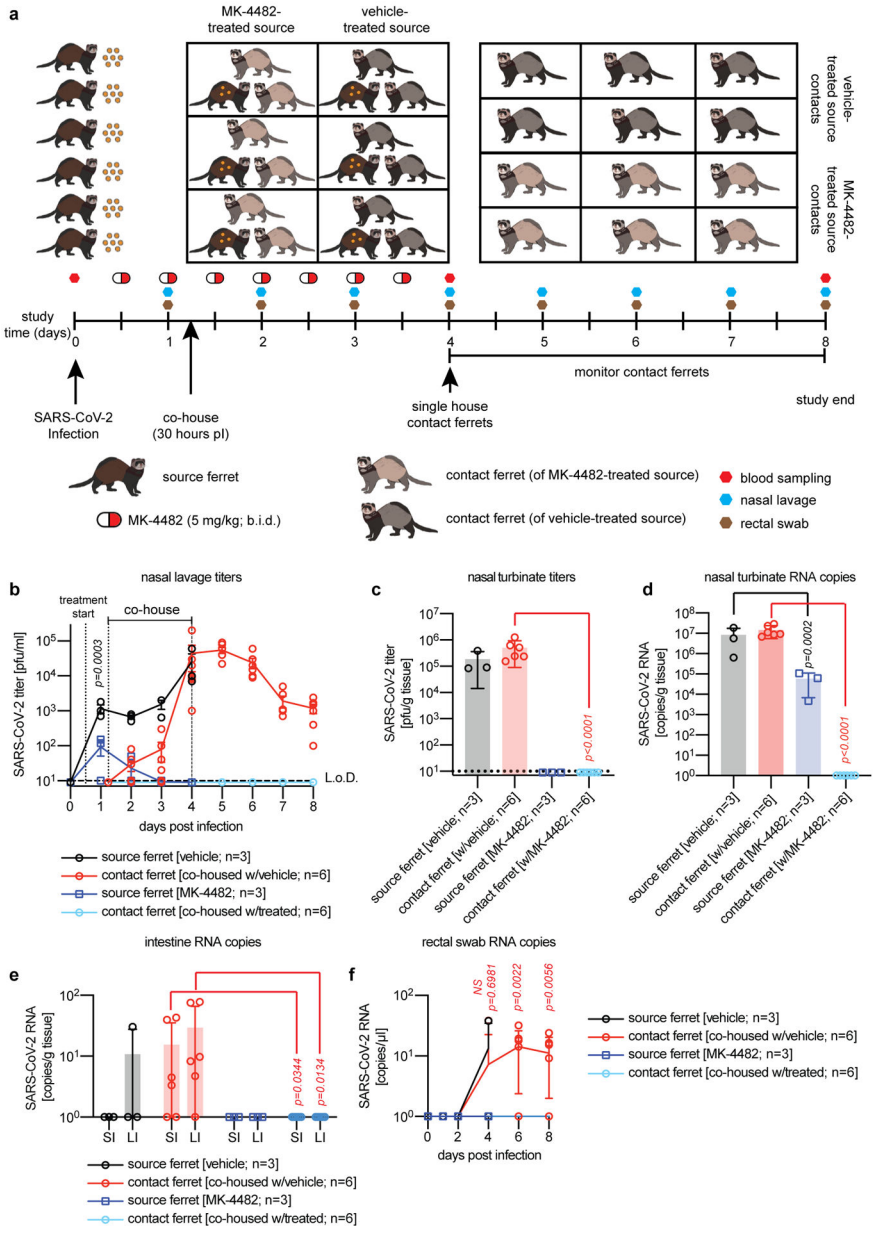

Fig. 3.

Therapeutic oral treatment with MK-4482/EIDD-2801 prevents contact transmission. **a,** Contact transmission study schematic. Two groups of source ferrets (n=3 biologically independent animals each) were infected with 1×10^5 pfu of 2019-nCoV/USA-WA1/2020 and received MK-4482/EIDD-2801 treatment (5 mg/kg *b.i.d.*; blue (b-f)) or vehicle (black (b-f)) starting 12 hours after infection. At 30 hours after infection, each source ferret was co-housed with two uninfected, untreated contact ferrets (light blue and red for MK-4482 treated or vehicle treated source ferrets, respectively (b-f)). After three days, source animals were euthanized and contact ferrets isolated and monitored for four days. Nasal lavages and rectal swabs were collected once daily and blood sampled at 0, 4, and 8 days post infection. **b**, Source ferrets treated with MK-4482/EIDD-2801 had significantly lower virus titers 12

hours after treatment onset (p=0.0003) than vehicle animals. Contacts of vehicle-treated sources began to shed 2019-nCoV/USA-WA1/2020 within 20 hours of co-housing. No virus was detectable in untreated contact of MK-4482/EIDD-2801-treated source ferrets. Statistical analysis by two-way ANOVA with Sidak's multiple comparison post-hoc test. P values are shown. **c-d,** Quantitation of infectious particles (c) and virus RNA copy numbers (d) in nasal turbinates of source and contact ferrets from (b), extracted four and eight days after study start, respectively. Statistical analysis by one-way ANOVA with Sidak's multiple comparison post-hoc test ($p<0.0001$ for intergroup comparison of contact animals (c); $p=0.0002$ and $p<0.0001$ for intergroup comparison of source and contract animals, respectively (d)). **e-f,** Quantitation of virus RNA copy numbers in small (SI) and large (LI) intestines (e) and rectal swabs (f). Samples of MK-4482/EIDD-2801-treated source ferrets and their contacts were PCR-negative for viral RNA. Statistical analysis by one-way (e) or two-way (f) ANOVA with Sidak's multiple comparison post-hoc test. Samples being compared in post-hoc tests (c-ef) are color coded black or red for vehicle treated source and contact ferrets, respectively). The number of independent biological repeats is shown for each subpanel. P values are shown. In all panels, symbols represent independent biological repeats (individual animals), lines connect group means ± SD (b,f), and bar graphs show means ± SD (c-e).